ENGINEERING TRANSACTIONS • Enging. Trans. • 40, 1, 81-102, 1992
Polish Academy of Sciences • Institute of Fundamental Technological Research

THERMAL PERFORMANCE OF TILTING-PAD JOURNAL BEARING

T. A. STOLARSKI (UXBRIDGE)

The results of studying, both theoretically and experimentally, the temperature profiles of tilting-pad journal bearing suggest that the heat transfer mechanism within the bearing has a significant effect on the thermal performance of the bearing and hence its overall performance. The heat transfer mechanism includes the heat transfer from the faces of the pads and the heat transfer occurring within the inter-pad cavities between the oil leaving the trailing edge of the pad and the shaft, and the cool supply oil. It is postulated that, in order to predict the performance of the bearing, it is necessary to couple computer modelling with experimental testing.

NOTATION

c	clearance,
c_v	specific heat capacity of lubricant,
h	film thickness,
G_θ, G_z	Hirs turbulence coefficients,
J	functional,
k	thermal conductivity,
L	bearing axial length,
m_i	preload, $1-(c_{bi}/c_{pi})$,
n	axial pressure exponent,
O	centre,
P	pressure,
Q	flowrate,
r, θ, z	cylindrical polar coordinates,
R	shaft radius,
R_2	outer radius of pads,
T	temperature,
U	shaft surface velocity,
x, y, z	Cartesian coordinates,
Y	non-dimensional film coordinate, y/h
α_i	pivot offset, $\bar{\theta}_{pi}/\theta_p$,

α_p pad expansion coefficient,
α_S shaft expansion coefficient,
γ local heat transfer coefficient,
Δ_i pad tilt,
ΔR_p change in pad radius,
ΔR_S change in shaft radius,
θ angle,
μ absolute viscosity,
ρ lubricant density,
τ_{corr} turbulence correction factor,
ω shaft angular velocity.

SUBSCRIPTS

A ambient,
av average,
b bearing,
cav cavitation,
ce centerline,
f fluid,
i pad number or trailing edge,
$i+1$ leading edge,
m mean,
0 reference,
p pad or pivot,
S shaft,
si supply.

1. INTRODUCTION

The advantage offered by the tilting-pad journal bearing consists in the lack of self-excited instability and, therefore, it is considered as suitable for high speed or lightly loaded turbomachinery. However, in comparison to fixed-geometry bearings it is a rather complex bearing to manufacture and analyse due to its multicomponent nature. In designing a tilting-pad journal bearing, one should choose the dimensions of the bearing such that the resulting operational characteristics of the bearing secure a stable rotor system. The stability of the rotor system often depends critically on the stiffness of a support and hence, in turn, on the stiffness of the bearings. The stiffness and damping properties of the bearing depend on the eccentricity of the rotor within the bearings and hence, on the thermohydrodynamic

performance of the bearing [1, 2]. Therefore, in order to predict rotor dynamic performance at the design stage, an accurate thermohydrodynamic analysis of the bearing is required.

A number of theoretical models of the tilting-pad journal bearing have been developed but none of them is in sufficient agreement with experimental data. Therefore, it is postulated in this paper that the proper approach to the problem is a close integration of a computer modelling with experimental results. Thus, in this paper, a theoretical model of the tilting-pad bearing developed in a way similar to that used by others [1, 2] is verified against experimental results and, as a result of that, ways to improve the predictived power and accuracy of the model are suggested.

2. Modelling of the tilting-pad journal bearing

2.1. The geometry

A characteristic feature of the tilting-pad journal bearing is that each of the bearing pads is pivoted. If the movement of the shaft within the bearing is defined in terms of the global coordinates (x, y), Fig.1, and the pitch angle of each pad by Δ_i, then the fluid film thickness associated with each pad is

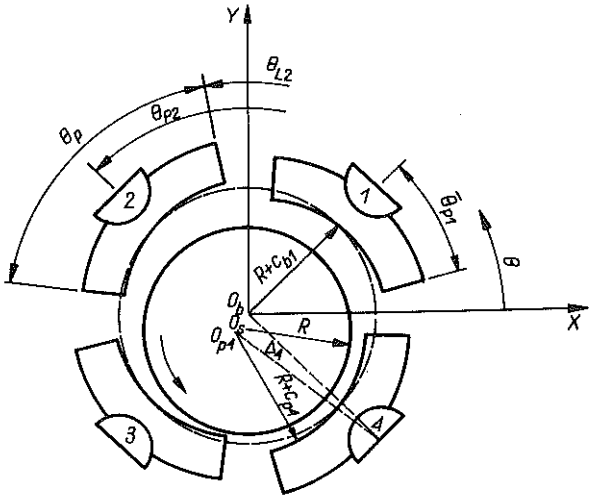

FIG. 1. Titling-pad journal bearing geometry.

given by

$$h_i = c_{pi} - x\cos\theta - y\sin\theta - m_i c_{pi}\cos(\theta_{pi} - \theta) + (R + c_{pi})\Delta_i \sin(\theta_{pi} - \theta), \tag{2.1}$$

where c_{pi} is the nominal clearance of i-th pad, θ is the running angle measured from x-axis (see Fig.1), θ_{pi} is the angle defining the position of i-th pad, R is the shaft nominal radius and m is preload defined as $(c_p - c_b)/c_p$. Preload factor, m, can be different for different pads.

2.2. Governing equations

The pressure generated within the lubricating film is given by the Reynolds equation

$$\frac{1}{R^2}\frac{\partial}{\partial\theta}\left(G_\theta \frac{h^3}{\mu}\frac{\partial P}{\partial\theta}\right) + \frac{\partial}{\partial z}\left(G_z \frac{h^3}{\mu}\frac{\partial P}{\partial z}\right) = \frac{\omega}{2}\frac{\partial h}{\partial\theta}, \tag{2.2}$$

where G_θ and G_z are turbulence correction factors derived by HIRS [3]. The accompanying boundary conditions are

$$P(\theta_l, z) = P(\theta_t, z) = P_S, \tag{2.3}$$

$$P\left(\theta, \pm\frac{L}{2}\right) = 0 \tag{2.4}$$

and at the location of cavitation the Reynolds boundary conditions are applied, i.e.

$$P_{\text{cav}} = 0, \qquad \left.\frac{\partial P}{\partial\theta}\right|_{\text{cav}} = 0. \tag{2.5}$$

The Reynolds equation (2.2) contains terms for viscosity. In the case of hydrodynamic lubrication, they can be considered to be only a function of temperature and can be evaluated once the film temperatures are known. The variation of viscosity with temperature is accurately modelled by VOGEL'S law [4]

$$\mu = a\exp\left(\frac{b}{T + t_c}\right), \tag{2.6}$$

where a, b and t_c are constant for a specific lubricant.

The film temperatures are obtained by solving a form of the energy equation. One form of the energy equation given by [5] is

$$\rho c_v \left[\left(\frac{Uh}{2} - \frac{h^3}{12\mu R}\frac{\partial P}{\partial \theta}\right)\frac{1}{R}\frac{\partial T}{\partial \theta} - \frac{h^3}{12\mu}\frac{\partial P}{\partial z}\frac{\partial T}{\partial z}\right] - k\left[\frac{1}{R^2}\frac{\partial}{\partial \theta}\left(h\frac{\partial T}{\partial \theta}\right) + \frac{\partial}{\partial z}\left(h\frac{\partial T}{\partial z}\right)\right] + k\left[\left.\frac{\partial T}{\partial y}\right|_{y=h} - \left.\frac{\partial T}{\partial y}\right|_{y=0}\right] = \mu\frac{U^2}{h} + \frac{h^3}{12\mu}\left[\frac{1}{R^2}\left(\frac{\partial P}{\partial \theta}\right)^2 + \left(\frac{\partial P}{\partial z}\right)^2\right]. \tag{2.7}$$

In this energy equation it is assumed that the fluid is incompressible and that variations in the fluid thermal properties c_v and k are negligible.

In order to calculate pad temperatures, the conduction equation given below ought to be solved together with the film energy equation (2.7)

$$\frac{\partial^2 T}{\partial r^2} + \frac{1}{r}\frac{\partial T}{\partial r} + \frac{1}{r^2}\frac{\partial^2 T}{\partial \theta^2} + \frac{\partial^2 T}{\partial z^2} = 0. \tag{2.8}$$

3. Approximate solution techniques

In the following, the approximate solution techniques that were used to solve the governing equations are described. Their effect was to simplify the equations so that simpler and computationally quicker methods could be used to solve them.

3.1. Approximate techniques for the solution of the Reynolds equation

Studies by a number of researchers [6 - 9] have outlined a method for simplifying the solution to the Reynolds equation whilst still retaining the pressure gradients in both the axial and circumferential directions. This is achieved by assuming the pressure distribution in the axial direction z to be a polynomial function of the centreline pressure, i.e.

$$P(\theta, z) = P_{ce}(\theta)\left[1 - \left|\frac{2z}{L}\right|^n\right]. \tag{3.1}$$

Ettles [1] undertook a numerical study and showed that, in order to reduce errors in comparison to two-dimensional solution, n should vary with the L/D ratio, in the following way:

$$n = 2 + 0.571\left(\frac{L}{D}\right)^{1.66}. \tag{3.2}$$

The Reynolds equation can be solved by various numerical methods. By applying the calculus of variations it has been shown [10] that the solution of the Reynolds equation minimises the functional

$$(3.3)\quad J(P) = \int_{\theta_i}^{\theta_t} \int_{-L/2}^{+L/2} \left\{ \frac{G_\theta h^3}{2R^2\mu} \left(\frac{\partial P}{\partial \theta}\right)^2 + \frac{G_z h^3}{2\mu} \left(\frac{\partial P}{\partial z}\right)^2 + \left(\frac{\omega}{2}\frac{\partial h}{\partial \theta}\right) P \right\} dz d\theta.$$

On substituting Eq.(3.1) for the pressure and integrating over the axial length the functional (3.3) becomes

$$(3.4)\quad J(P) = \int_{\theta_i}^{\theta_t} \left\{ \frac{G_\theta h^3}{2R^2\mu} \left(\frac{L}{2} - \frac{L}{n+1} + \frac{L}{2(2n+1)}\right) \left(\frac{\partial P_{ce}}{\partial \theta}\right)^2 + \frac{G_z h^3}{\mu} \frac{2n^2}{L(2n-1)} P_{ce}^2 + \frac{\omega}{2}\frac{\partial h}{\partial \theta} \left(L - \frac{L}{n+1}\right) P_{ce} \right\} d\theta.$$

This functional was solved by a finite element technique, similar to that outlined in [10], to obtain the solution to Reynolds equation. The details of both the finite element method and the procedures used can be found in [11].

3.2. Approximate techniques for the solution of the energy equation

The energy equation (2.7) includes conduction within the film. The circumferential and axial conduction terms were considered to be small in comparison to the cross-film conduction term and so, in this analysis they were omitted. By substituting the expression (3.1) for pressure into the energy equation (2.7) the following expression for the temperature gradient in the circumferential direction can be obtained:

$$(3.5)\quad \frac{\partial T}{\partial \theta} = \frac{\mu \dfrac{U^2}{h} + \dfrac{h^3}{12\mu R^2} \left(\dfrac{\partial P_{ce}}{\partial \theta}\right)^2 - k \left[\left.\dfrac{\partial T}{\partial y}\right|_{y=h} - \left.\dfrac{\partial T}{\partial y}\right|_{y=0} \right]}{\dfrac{\rho c_v}{R} \left(\dfrac{Uh}{2} - \dfrac{h^3}{12\mu R} \dfrac{\partial P_{ce}}{\partial \theta} \right)}.$$

The film temperatures are obtained from (3.5) by using a marching technique, once the film temperature boundary condition at the leading edge of the pad is set. The temperature gradients in the conduction term in Eq.(3.5)

are obtained by assuming that the temperature distribution across the film can be approximated by a 2-nd order polynomial [10],

$$T = A + BY + CY^2, \tag{3.6}$$

where $Y = y/h$. The terms A, B and C can be found by applying the conditions that

$$T(Y=0) = T_b, \tag{3.7}$$

$$T(Y=1) = T_S, \tag{3.8}$$

$$\int_{Y=0}^{Y=1} \frac{\partial T}{\partial Y} dY = T_m, \tag{3.9}$$

and the result is a cross-film temperature distribution of the form

$$T = T_b + 2(3T_m - T_S - 2T_b)Y + 3(T_S - 2T_m + T_b)Y^2. \tag{3.10}$$

On substituting Eq.(3.10) for temperature into Eq.(3.5) the energy equation becomes

$$\frac{\partial T}{\partial \theta} = \frac{\mu \dfrac{U^2}{h} + \dfrac{h^3}{12\mu R^2}\left(\dfrac{\partial P_{ce}}{\partial \theta}\right)^2 - \dfrac{6k}{h}(T_S - 2T_m + T_b)}{\dfrac{\rho c_v}{R}\left(\dfrac{Uh}{2} - \dfrac{h^3}{12\mu R}\dfrac{\partial P_{ce}}{\partial \theta}\right)}. \tag{3.11}$$

3.3. Approximate techniques for the solution of the pad conduction equation

The experimental results [12, 13] indicate that the axial temperature variation in an aligned bearing is small. On the basis of these results, the axial term in the pad conduction equation can be neglected. To simplify the analysis even further and to reduce computation time, the conduction term in the circumferential direction is also neglected. The pad conduction equation then reduces to

$$\frac{\partial^2 T}{\partial r^2} + \frac{1}{r}\frac{\partial T}{\partial r} = 0. \tag{3.12}$$

This reduced equation has an analytical solution of the form

$$T = a_0 + b_0 \ln r. \tag{3.13}$$

The boundary conditions applicable in this model are

$$k_f \left.\frac{\partial T}{\partial y}\right|_{y=0} = k_b \left.\frac{\partial T}{\partial r}\right|_{r=R}, \tag{3.14}$$

$$k_b \left.\frac{\partial T}{\partial r}\right|_{r=R_2} = -\gamma(T - T_A), \tag{3.15}$$

where R_2 is the radius of the back surface of the pads and T_A is the temperature of the fluid behind the pads. Condition (3.14) ensures that heat flux is continuous at the fluid-pad interface. In a conventionally lubricated tilting-pad journal bearing oil floods the cavity behind the pads. It is therefore thought that the heat convection boundary condition, given by Eq. (3.15) is more appropriate than the fixed temperature boundary condition used in [2]. By applying the boundary conditions to Eq. (3.13) and using Eq. (3.6) an expression for pad temperature can be obtained,

$$T = T_b - R_2 \frac{\gamma}{k_b}[T_{R_2} - T_A] \ln\left(\frac{r}{R}\right). \tag{3.16}$$

As can be seen, the energy equation (3.11) for the film and the pad conduction equation (3.12) are coupled via the pad surface temperature T_b. So in practice, they are solved iteratively until the temperatures stabilise.

3.4. Calculation of operating clearances

In operation, the clearances within the tilting-pad bearing change due to the thermal expansion of the bearing components [14, 15]. The shaft expands outwards and so reduces the pad and bearing clearances, c_p and c_b, respectively. This expansion is normally calculated using the following formula:

$$\Delta R_S = \alpha_S R(T_S - T_0). \tag{3.17}$$

The pads of the tilting-pad journal bearing also expand. However, the way and the amount by which they expand, depend upon the type of pivot used. Neglecting the pivot, an approximate value for the pad expansion can be obtained from

$$\Delta R_p = \alpha_p \left[R \exp\left[\frac{k_b}{\gamma R_2}\frac{(T_{\mathrm{av}} - T_{\mathrm{avp}})}{(T_{R_2} - T_A)}\right] - R\right](T_{\mathrm{avp}} - T_0), \tag{3.18}$$

where T_{av} is the average surface temperature of the pad and T_{avp} is the average pad temperature. In the approximation (3.18) it is assumed that the pad expands about the radius at which the average pad temperature occurs; this may be considered to be the axis of neutral thermal expansion.

3.5. Calculation of the leading edge mean film temperature

As yet the problem of calculating the leading edge film temperature accurately for any particular bearing and operating condition has not been resolved, although many papers on this topic have been published [16-22].

The most widely used model is that of "groove mixing theory" [17], in which the mean film temperature at the leading edge T_{i+1} is calculated from the heat-flow balance,

$$T_{i+1}Q_{i+1} = T_iQ_i + T_{si}\Delta Q\,, \tag{3.19}$$

where

$$\Delta Q = (Q_{i+1} - Q_i)\,.$$

In [16, 18, 19], the above equation is modified to allow for "groove effects" such as heat transfer and the loss of hot oil. Values for these effects are either found from experiment or they are reasoned. In this model the "groove-mixing" theory of LUND [16] is used as it allows the heat transfer effects to vary from groove to groove. In Lund's theory the mean film temperature at the leading edge of the pad is given by

$$T_{i+1}Q_i = Q_i[(T_i - \gamma_1(T_i - T_S) - \gamma_2(T_i - T_{si})] + \begin{cases} \Delta QT_{si} & (\Delta Q > 0)\,, \\ \Delta QT_{i+1} & (\Delta Q < 0)\,. \end{cases} \tag{3.20}$$

3.6. Calculation of the shaft temperature

Published experimental results [12, 13, 23] indicate that the shaft can be considered as an isothermal element under laminar conditions, because temperature variations in the axial and circumferential directions within the shaft are small. These experimental results also indicate that the average bearing surface temperature is a good estimate of the shaft temperature. A better estimate may be the average bearing film temperature, and so in this model it is used as an approximation to the shaft temperature,

$$T_S = \frac{1}{2\pi}\int_0^{2\pi} T_m\, d\theta\,. \tag{3.21}$$

3.7. Program structure

All the above elements have been incorporated into a computer program in order to obtain bearing temperatures, pressures, film thicknesses, power losses and oil flowrates. A flowchart of the program is given in Figure 2.

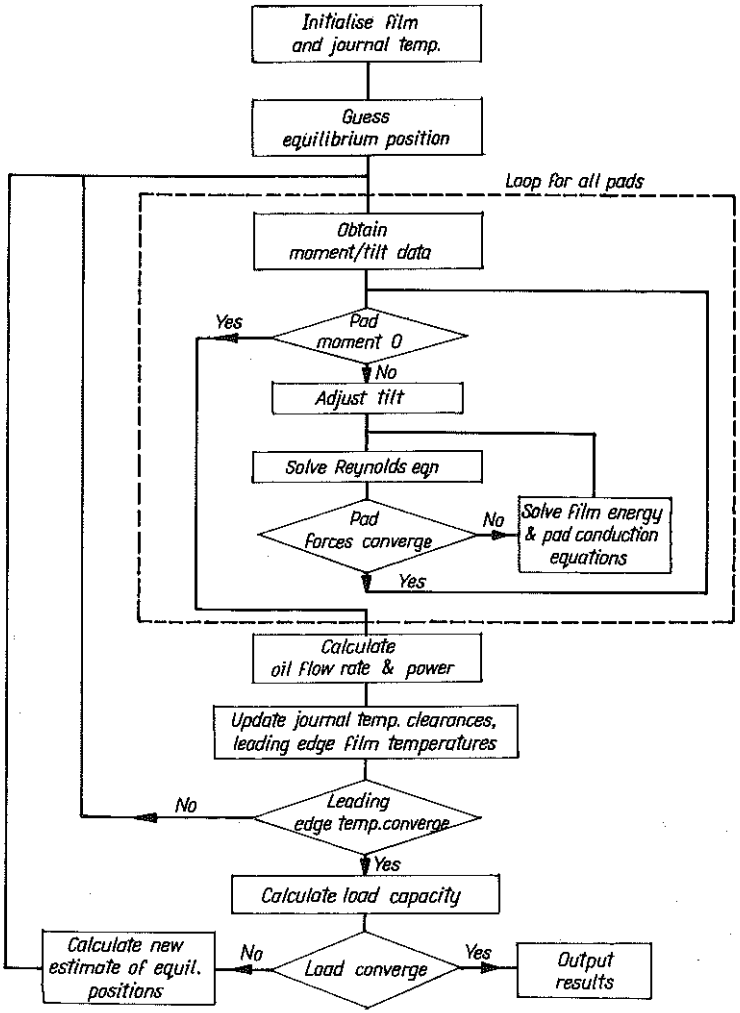

FIG. 2. Program flow-diagram.

4. MODEL VERIFICATION

4.1. Comparison with Brockwell and Kleinbub

Recently BROCKWELL and KLEINBUB [24] presented experimental data for 5 pad tilting-pad journal bearings. Two bearings with different L/D ratios were tested, one with an L/D ratio of 0.46 and the other with an

L/D ratio of 0.75. Input data used by the program to produce results for comparison with experiment are given in Table 1.

Table 1. Calculation data for the Brockwell and Kleinbub bearing.

Bearing type	5 pad tilting-pad bearing
Diameter	76 mm
Length	35 and 57 mm
Bearing clearance	0.120 mm
Preload	0.0
Offset	0.50
Pad arc length	54 °
Groove	18 °
Pad thickness	16 mm
Load direction	between pads
Pad thermal conductivity	50 W/m°C
Oil temperature behind pads	50.0 °C
Pad pack surface heat transfer coefficient	100 W/m^2 °C
Groove mixing coefficients	0.05
Oil properties	
Oil	ISO VG 32
Absolute viscosity	0.02787 Pas at 40 °C
	0.00467 Pas at 100 °C
Density	871 kg/m^3
Specific heat	1952 J/kg°C
Thermal conductivity	0.15 W/m°C
Oil supply temperature	50.0 °C
Oil supply flowrate	0.07 l/s
Oil supply pressure	45 kPa (0.75 L/D)
	75 kPa (0.46 L/D)

Results for bearing surface temperatures for the bearing with the L/D ratio of 0.46, at two different speeds, are given in Figure 3. Theoretical temperatures agree quite well with experimental values at 1800 rpm, although the theory consistently overpredicts experiment. At 9000 rpm, theory again overpredicts temperatures but now the difference between the theoretical values and the experimental values is greater. In the loaded pads 1 and 2, the model cannot predict the temperature drop in the trailing edges of the pads. This temperature drop appears to be due to heat transfer from the hot trailing edge region to the cool supply oil in the inter-pad cavity. In the

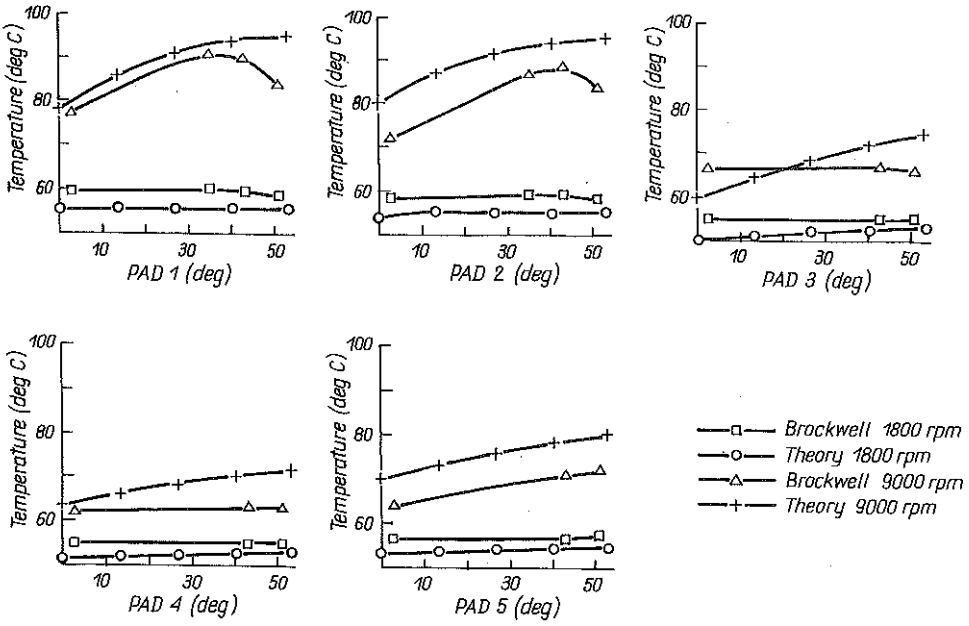

FIG. 3. Comparison of bearing surface temperatures; bearing: Brockwell 5 pad tilting-pad journal bearing; load: 5520; N L/D: 0.46.

unloaded pads, the main discrepancy between theory and experiment is in the values of the temperature gradients.

In Figure 4 bearing surface temperatures are presented for the bearing with the L/D ratio of 0.75, again at two different speeds. The results of comparison between experiment and theory are very similar to those for the bearing with the L/D ratio of 0.46. The only notable difference is that at 1800 rpm the theoretical temperatures underestimate rather than overestimate experimental temperatures.

At the 9000 rpm condition, Figs.3 and 4, the discrepancies between theory and experiment are rather too large to inspire confidence in the model. In addressing this problem it was instructive to look at the oil supply flowrates. The calculated and experimental flowrates are shown in Tables 2 and 3.

As can be seen from the tables, the amount of oil required to produce a complete hydrodynamic film, as calculated by the program, is much less than that supplied to the bearing during the experimental tests. In the paper [24], graphs showing the effect of oil supply flowrates on maximum bearing temperatures are presented. These graphs are reproduced in Fig.5.

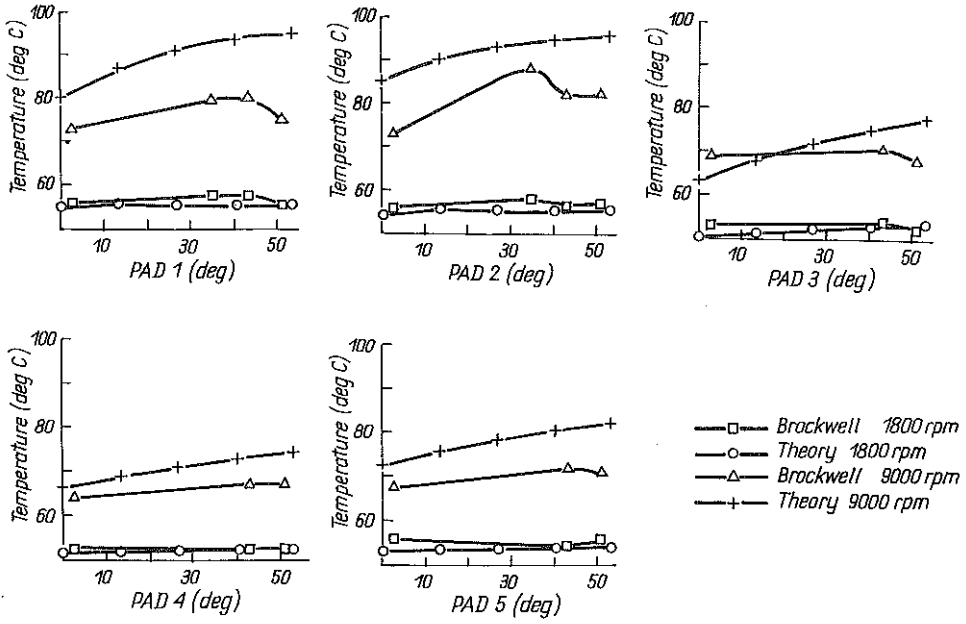

FIG. 4. Comparison of bearing surface temperatures; bearing: Brockwell 5 pad tilting-pad journal bearing; load: 8900 N; L/D: 0.75.

Table 2. Oil supply flowrates for the L/D 0.46 bearing.

Conditions	1800 rpm 5520 N		9000 rpm 5200 N	
	Exp.	Theory	Exp.	Theory
Oil flowrate (l/s)	0.07	0.0088	0.07	0.0118

As can be seen from this figure, maximum bearing temperatures increase as the oil supply flowrate is reduced. Even allowing for oil leakage within the bearing assembly, the calculated oil flowrate will probably still be less than the experimental flowrate, which would therefore explain most of the discrepancies in bearing temperatures between theory and experiment. An interesting question related to the tilting-pad journal bearing is, why do maximum bearing temperatures increase if the oil supply flowrate is reduced. There appear to be two main reasons. The first is that a reduced oil flowrate through the bearing leads to lower convected heat loss from the sides and back surfaces of the pads. The second reason is that the oil supplied at the reduced flowrate may not influence the temperature of the oil forming the hydrodynamic film as effectively as when it is supplied at higher flowrates.

Table 3. Oil supply flowrates for the L/D 0.75 bearing.

Conditions	1800 rpm 8900 N		9000 rpm 8900 N	
	Exp.	Theory	Exp.	Theory
Oil flowrate (l/s)	0.07	0.009	0.07	0.012

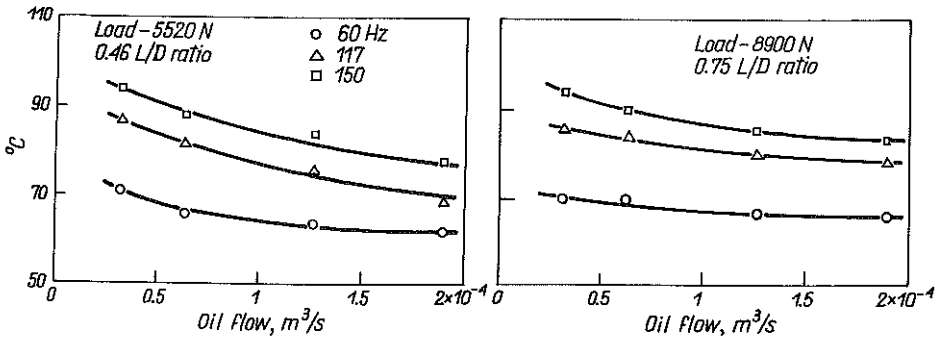

FIG. 5. Effect of oil flow on maximum bearing temperatures.

Referring to the first reason and the value of the heat transfer coefficient of 100 W/m^2°C used in the program, the question arises, what flowrate of oil gives rise to this value for the heat transfer coefficient? Due to the lack of experimental work in this area, this question cannot at present be answered. However, if the above value for the heat transfer coefficient is less than that in experiment then the program may model experiment quite well. Regarding the second reason, values for the heat transfer coefficients in the groove mixing equation (3.20) need to be obtained to allow the modelling of the variation leading edge film temperatures with oil supply flowrate. It should also be noted that the leading edge temperatures of pad 1 are equal to or higher than the trailing edge temperatures of pad 5. This seems to indicate that heat transfer occurs from the shaft to the oil film leaving the trailing edge of pad 5.

4.2. Comparison with Fillon end Frene

Results from the model were also compared with the experimental results obtained for a 4 pad journal bearing by FILLON and FRENE [25]. The bearing data input into the program are given in Table 4.

Table 4. Calculation data for the Fillon and Frene bearing.

Bearing type	4 pad tilting-pad bearing
Diameter	100 mm
Length	70 mm
Bearing clearance	0.074 mm (2000 rpm, 1000 N)
	0.066 mm (4000 rpm, 1000 N)
Preload	0.50 (2000 rpm, 1000 N)
	0.54 (4000 rpm, 1000 N)
Offset	0.50
Pad arc length	75 °
Groove	15 °
Pad thickness	20 mm
Load direction	between pads
Pad thermal conductivity	50 W/m°C
Oil temperature behind pads	40.0 °C
Pad back surface heat transfer coefficient	100 W/m^2 °C
Groove mixing coefficients	0.05
Oil properties	
Absolute viscosity	0.0277 Pas at 40 °C
	0.00467 Pas at 100 °C
Density	871 kg/m^3
Specific heat	1952 J/kg°C
Thermal conductivity	0.15 W/m°C
Oil supply temperature	40.0 °C
Oil supply pressure	50 kPa

In the paper, operating clearances were presented which were calculated from the measured bearing temperatures and therefore there was no need to include the modelling of the thermal expansion of the shaft and pads in the program.

Experimental and theoretical results for pad surface temperatures are presented in Figs.6 and 7 at a load of 1000 N. At 2000 rpm, Fig.6, it is seen that the theoretical temperatures overpredict experimental temperatures in all pads, though the temperature gradients are correct. At 4000 rpm, Fig.7, the results of comparison are very similar to those at 2000 rpm. In both Figs.6 and 7, the experimental bearing surface temperatures are presented at two different flowrates. The figures show that the bearing surface temperatures increase but the temperature gradients remain the same as the

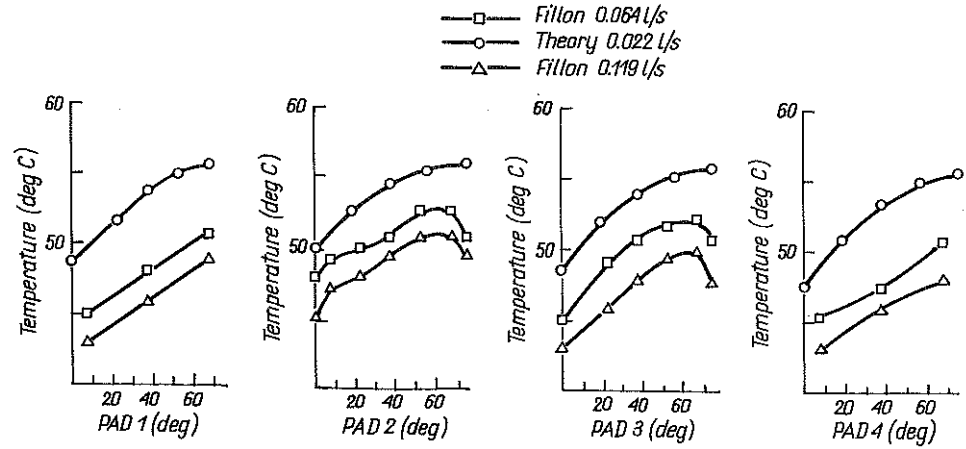

FIG. 6. Comparison of bearing surface temperatures; bearing: Fillon and Frene 4 pad tilting-pad journal bearing; load: 1000 N; speed: 2000 rpm.

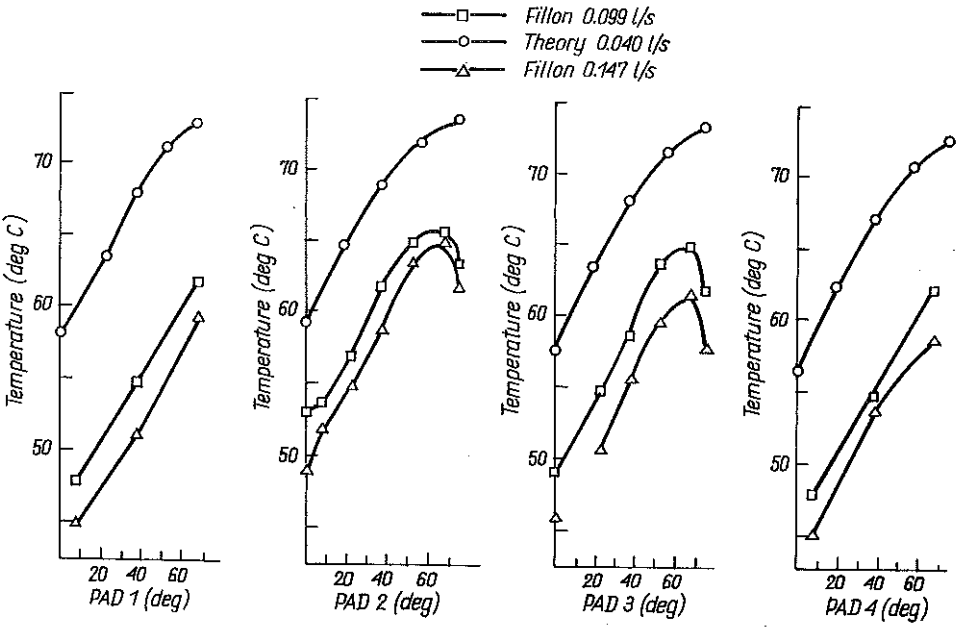

FIG. 7. Comparison of bearing surface temperatures; bearing: Fillon and Frene 4 pad tilting-pad journal bearing; load: 1000 N; speed: 4000 rpm.

oil supply flowrate is decreased. At both 2000 rpm and 4000 rpm, the program calculated the required oil supply flowrate to be much lower than that actually supplied during the experiments. This would appear to account for most of the discrepancy between the experimental bearing surface tempera-

tures and those calculated by the program.

An interesting finding emerging from the work of Fillon and Frene is that the shaft temperature should not be estimated by the average bearing surface temperature. This is evident on studying Figs.6, 7 and Fig. 8 which is reproduced from [25]. If the experimental measurements are reliable then

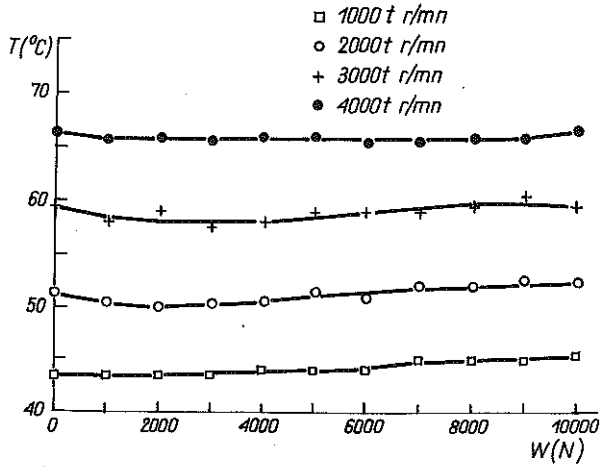

FIG. 8. Maximum shaft surface temperatures.

it appears that at 4000 rpm the maximum shaft temperature is almost the same as the maximum bearing surface temperature.

4.3. Comparison with experiment

In a study of the effects of lubrication methods on the performance of the tilting-pad journal bearing [26], pad temperatures were obtained for a 4 pad tilting-pad bearing. Input data required for the program are given in Table 5.

It should be noted that the thermal conductivity of the bronze from which the pads were made was not measured and so the value of 250 W/m°C is only an estimate and could easily be in error by 50 W/m°C. It should also be noted that even though the oil inlet pressure remained zero throughout the experimental tests, the bearing never ran under starved conditions.

Results for bearing temperatures are presented for two different load conditions in Figs.9 and 10. At the lowest load condition, Fig.9, theoretical predictions agree well with experiment at 1671 rpm; however, at 7745 rpm

Table 5. Calculation data for the experimental bearing.

Bearing type	4 pad tilting-pad bearing
Diameter	127 mm
Length	127 mm
Bearing clearance	0.2032 mm
Preloads	pad 1 -0.772
	pad 2 -0.299
	pad 3 -0.722
	pad 4 -0.949
Offset	0.50
Pad arc length	72 °
Groove	18 °
Pad thickness	38.1 mm
Load direction	between pads
Pad thermal conductivity	250 W/m°C
Pad back surface heat transfer coefficient	100 W/m^2 °C
Pad expansion coefficient	1.1394E-5/°C
Shaft expansion coefficient	1.8E-5/°C
Groove mixing coefficients	0.05
Oil properties	
Oil	Shell Tellus 37
Absolute viscosity	0.0575 Pas at 20°C
	0.0085 Pas at 68°C
Density	865 kg/ms 403
Specific heat	1952 J/kg°C
Thermal conductivity	0.15 W/m°C
Oil supply temperature	40°C
Oil supply flowrate	0.4 l/s
Oil inlet pressure	0.0 kPa

there exist a number of discrepancies. At this speed, temperature predictions for pad 1 are reasonable but for pad 2 the leading edge temperature is too high, though the temperature gradient is acceptable. Regarding pads 3 and 4, the theoretical leading edge temperetures are correct but the theoretical temperature gradients are too shallow.

In Fig.10, pad temperatures are presented at the highest load condition. At this condition the temperature trends are very similar to those observed at the lightest load, Fig.9.

The large discrepancy in leading edge temperature for pad 2 at both load conditions is rather surprising. Assuming that no computational error

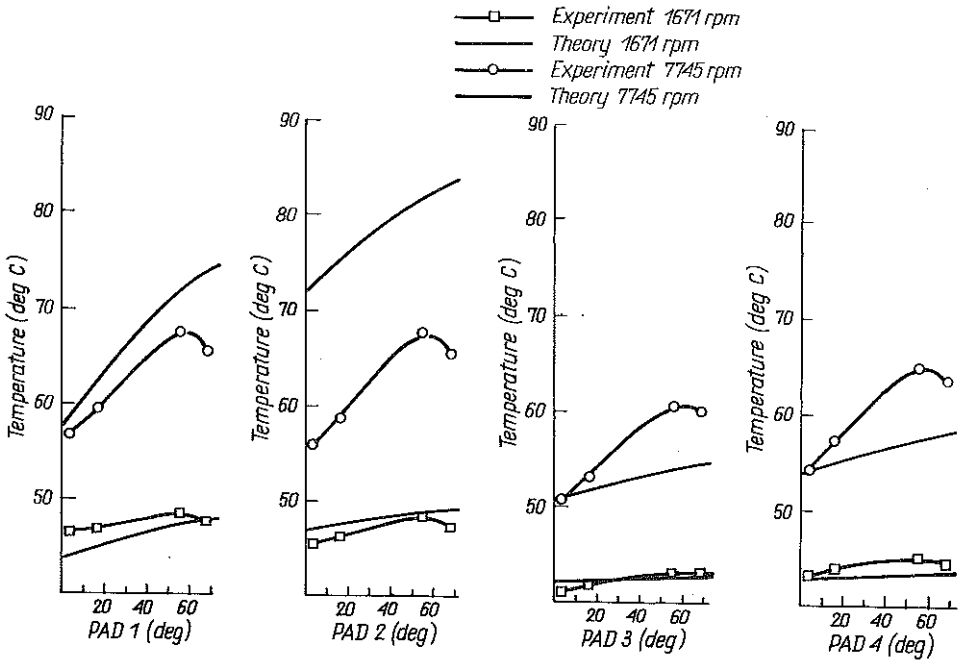

FIG. 9. Comparison of bearing surface temperatures; bearing: Flooded 4 pad tilting-pad bearing; load: 3394 N; flowrate: 0.4 l/s.

has been made then it appears that a significant amount of heat transfer occurs from the fluid film leaving the trailing edge of pad 1 to the shaft and the oil in the inter-pad cavity as it traverses the inter-pad cavity. In the case of pads 3 and 4, the "groove mixing" theory appears to predict leading edge temperatures well, however the temperature gradients are too shallow and indicate that the clearances predicted for these pads are too large. The magnitude of the temperature drop in the trailing edge regions of the loaded pads also indicate the necessity of two-dimensional modelling of the bearing pads to take into consideration heat losses through the end faces of the pads. As with the bearing in [24], it is seen that in most circumstances the temperature of the first loaded pad, pad 1, is higher than the trailing edge temperature of the previous pad, pad 4. Again this indicates that heat transfer occurs from the shaft to the oil film leaving the trailing edge of pad 4.

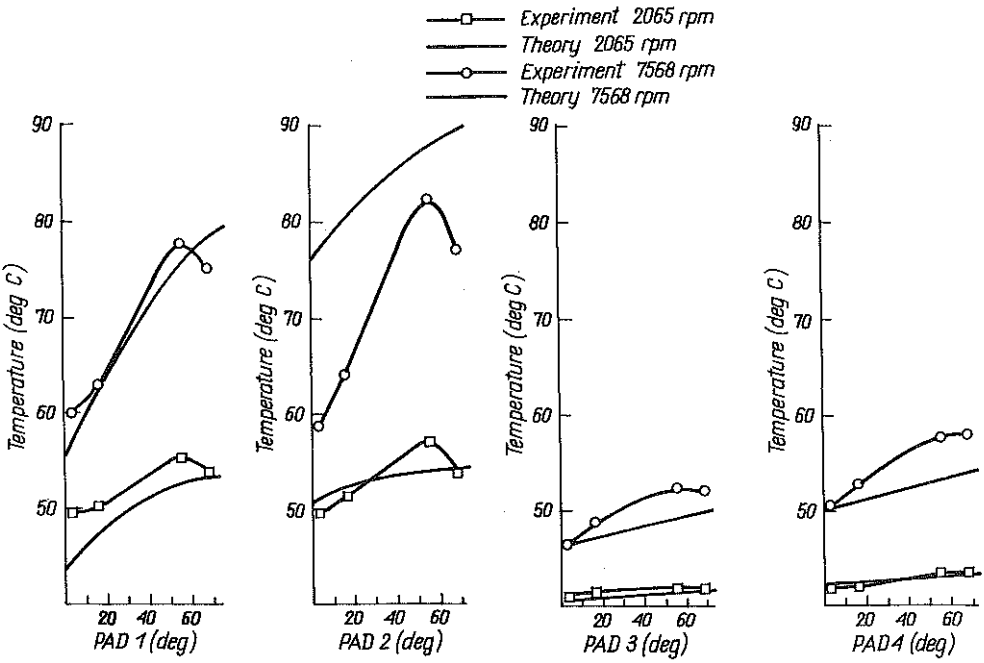

FIG. 10. Comparison of bearing surface temperatures; bearing: Flooded 4 pad tilting-pad bearing; load: 21187 N; flowrate: 0.4 l/s.

5. CONCLUSIONS

A program based on a model which uses approximate techniques to solve the Reynolds film energy equation and pad conduction equations has been developed to aid the design and optimisation of tilting-pad journal bearings. In comparing progam results against published experimentel results, it has become apparent that a good estimate of the heat transfer coefficient for the back surface of the pads is essential, if the program is to produce acceptable results. This conclusion stems from the observation that the oil supply flowrate affects the temperatures within the bearing.

It has also been observed that heat transfer seems to occur between the oil leaving the trailing edge of the pads and the shaft and the cool supply oil. Again this phenomenon needs to be studied experimentally to obtain values for the heat transfer coeffcients.

Heat transfer also occurs through the end faces of the pads. In order to model this the pad heat conduction equation must include both radial and circumferential conduction. Together with this, values for the corresponding

heat transfer coefficients need to be measured.

Heat transfer mechanisms significantly affect the thermal performance of the tilting-pad journal bearing and hence the overall characteristics of the bearing. Hence in order to improve the modelling of the tilting-pad journal bearing the above heat transfer effects need to be studied experimentally in greater detail.

REFERENCES

1. C.M.McC.ETTLES, *The analysis and performance of pivoted pad journal bearings considering thermal and elastic effects*, Trans, ASME, J. Lubr. Trib., **102**, pp. 182-193, 1980.
2. J.D.KNIGHT, *Non-adiabatic thermal effects in tilting-pad and multilobe journal bearings*, PhD Thesis, Univ. of Virginia, January 1986.
3. G.G.HIRS, *A bulk-flow theory for turbulence in lubricating films*, Trans. ASME, J. Lubr. Techn., **95**, pp. 137-146, 1973.
4. A.CAMERON, *Basic lubrication theory*, E. Horwood Ltd., 1976.
5. O.PINKUS and B.STERNLICHT, *Theory of hydrodynamic lubrication*, McGraw-Hill, New York 1961.
6. J.P.O'DONOGHUE, P.R.KOCK and C.J. HOOKE, *Approximate short bearing analysis and experimental results obtained using plastic bearing liners*, 8th Tribology Conv. Proc., I Mech. Proc. vol. 184, Pt. 3L, 1970.
7. E.A.MOSS and B.W.SKEWS, *A solution to Reynolds equation as applied to journal bearings by reduction to an ordinary differential equation*, Adv. in Trib., I Mech. Tribology Conv., Durham 1976, MEP 1978.
8. W.R.JONES, *Rapid solutions to Reynolds equation with application to fluid film bearings*, Masters Thesis, Univ. of Virginia, 1980.
9. P. SHELLEY and C.M.McC.ETTLES, *A tractable solution for medium length journal bearings*, Wear, **12**, pp. 221-228, 1970.
10. J.D.KNIGHT and L.E.BARRETT, *An approximate solutions technique for multi-lobe journal bearings including thermal effects, with comparison to experiment*, ASLE Trans., **26**, 4, pp. 501-508, 1983.
11. P.E.ALLAIRE, *Basics of the finite element method, solid mechanics heat transfer and fluid mechanics*, W. C. Brown Publ., Iowa 1985.
12. D.DOWSON, J.D.HUDSON, B.HUNTER and C.N.MARCH, *An experimental investigation of the thermal equilibrium of steady loaded journal bearings*, J. Bear. for Reciproc. Turbo Mach., IMechE Proc., **181**, 3B, pp. 70-80, 1966-67.
13. J.MITSUI, Y.HORI and M.TANAKA, *The experimental investigation on the temperature distribution in circular journal bearings*, Trans. ASME, J. Trib., **108**, pp. 621-627, October 1986.

14. L.MALCHER, *Die Federungs und Damfungseigenschaften von Gleitlargern fur Turbomachinen*, Dipl.-Ing. Thesis, Karlsruhe Technische Hochschule, 1985.

15. D.BRUGIER and M.T.PASCAL, *Influence of elastic deformations of turbo-generator tilting-pad bearings on the static behaviour and on the dynamic coefficients in different designs*, Trans, ASME, **111**, pp. 364-371, 1989.

16. J.W.LUND and P.K.HANSEN, *An approximate analysis of the temperature conditions in a journal bearing. Part I. Theory*, Trans. ASME, **106**, pp. 228-236, 1984.

17. C.M.McC.ETTLES, *Hot oil carry-over in thrust bearings*, I. Mech. Conf. on Lubrication and Wear, 1970.

18. H.HESHMAT and O.PINKUS, *Mixing inlet temperatures in hydrodynamic bearings*, Trans. ASME, J. Trib., **108**, pp. 231-248, April 1986.

19. J.MITSUI, Y.HORI and M. TANAKA, *Thermohydrodynamic analysis of cooling effect of supply oil in circular journal bearings*, Trans. ASME, **105**, pp. 414-421, July 1983.

20. J.H.VOHR, *Prediction of the operating temperature of thrust bearings*, Trans. ASME, J. Trib., **103**, pp. 97-106, January 1981.

21. P.B.NEAL, *Infiuence of film inlet conditions on the performance of fluid film bearings*, J. Mech. Eng. Sci., **12**, 2, pp. 153-155, 1970.

22. D.T.GETHIN, *A finite element approach to analysing thermohydrodynamic lubrication in journal bearings*, Trib. Intern., **21**, pp. 67-75, April 1988.

23. A.O.ANDRISANO, *An experimental investigation on the rotating journal surface temperature distribution in a full circular bearing*, Trans. ASME, J. Trib., **110**, pp. 638-645, October 1988.

24. K.R.BROCKWELL and D.KLEINBUB, *Measurement oi the steady-state operating characteristics of the five-shoe tilting-pad journal bearing*, STLE Trib., Trans., **32**, 2, pp. 267-275, 1989.

25. M.FILLON, J.FRENE and R.BONCOMPAIN, *Étude experimentale de l'effet thermique dans les paliers oscillants*, Congres Intern. de Tribologie, Eurotrib 85, Lyon 1985.

26. A.V.HARANGOZO, *An investigation into the effects of lubrication methods on the performance of the tilting-pad journal bearing*, PhD. Thesis, Department of Mechanical Engineering, Brunel University, Uxbridge, U.K., March 1990.

DEPARTMENT OF MECHANICAL ENGINEERING
BRUNEL UNIVERSITY, UXBRIDGE, MIDDX, UNITED KINGDOM.

Received April 23, 1991.